Nanoscale Advances

REVIEW

View Article Online
View Journal | View Issue

Cite this: *Nanoscale Adv.*, 2024, **6**, 4309

Polyimide as a biomedical material: advantages and applications

Junjie Shu,[a] Zhongfu Zhou,[b] Huaping Liang*[a] and Xia Yang *[a]

Polyimides (PIs) are a class of polymers characterized by strong covalent bonds, which offer the advantages of high thermal weight, low weight, good electronic properties and superior mechanical properties. They have been successfully used in the fields of microelectronics, aerospace engineering, nanomaterials, lasers, energy storage and painting. Their biomedical applications have attracted extensive attention, and they have been explored for use as an implantable, detectable, and antibacterial material in recent years. This article summarizes the progress of PI in terms of three aspects: synthesis, properties, and application. First, the synthetic strategies of PI are summarized. Next, the properties of PI as a biological or medical material are analyzed. Finally, the applications of PI in electrodes, biosensors, drug delivery systems, bone tissue replacements, face masks or respirators, and antibacterial materials are discussed. This review provides a comprehensive understanding of the latest progress in PI, thereby providing a basis for developing new potentially promising materials for medical applications.

Received 7th April 2024
Accepted 3rd July 2024

DOI: 10.1039/d4na00292j

rsc.li/nanoscale-advances

1. Introduction

Even after decades of research in materials science and tissue engineering, creating functional human tissue models for the complete repair of organ functions *in vivo* and *in vitro* is still challenging. A large number of materials and technologies have been designed, investigated, and manufactured, but only few have been successfully applied in the clinic. To achieve successful translation of medical materials to clinical practice, the ideal characteristics of these materials include the ability to mimic the native organ structure and function; no toxicity; perfect integration into and interaction with tissues; and adaptation of the morphology and function of the organism, including sufficient vascular supply, no thrombus as well as active response to challenging environments, such as cancer, inflammation, and infection.[1] Therefore, an increasing number of investigations focusing on medical materials have been designed based on some directional improvements that can rescue the functions of organs and tissues.

Currently, the successful application of medical materials such as intraocular lenses,[2] poly(4-methyl-1-pentene) (PMP) artificial lung membranes for extracorporeal membrane oxygenation (ECMO),[3] and filtration membranes for continuous renal replacement therapies (CRRTs)[4] has provided groundbreaking solutions to choke points in related fields with the rapid development of medical devices; moreover, the demand for some of these medical materials is considerable. For example, more than 7–20 million candidates require lens implants annually worldwide.[5] The cost of ECMO therapy for treating adult patients diagnosed with acute respiratory distress syndrome is high, at approximately $98 784 116.[6] A total of 68% of 100 000 ECMO survivors are treated at more than 300 centers worldwide,[6] and ECMO has been proven to be an effective approach for saving the lives of these patients. The global market of hemostatic material was valued at USD 20.8 billion in 2022 and is predicted to progressively increase at a compound annual growth rate of 5.4% from 2022 to 2027.[7] This situation worldwide encourages academics as well as pharmaceutical and medical dressing and equipment industries to investigate more new products for the treatment of these diseases. However, in some cases, the properties of these materials cannot meet the clinical requirements for complex pathological conditions *in vivo*. For example, artificial blood vessels that can be implanted for a long time in the body without adverse reactions, such as thrombosis caused by lower limb ischemia, are lacking.[8] The oxidized cellulose-based commercial hemostatic material Surgicel® is highly effective in blocking minor arterial bleeding and reducing intracranial hematoma in bleeding patients. However, the acidic microenvironment can potentially induce an inflammatory response, delaying the wound-healing process and damaging peripheral nerves.[9] An effective way to improve the functions and overcome the shortcomings of these materials is to develop composite materials, which provide a new hope for expanding the application range of single biomaterial in the medical field. For example, chitosan combined with quaternary ammonium groups exhibited improved antibacterial properties.[10] Another way is to

[a]*Department of Wound Infection and Drug, State Key Laboratory of Trauma and Chemical Poisoning, Daping Hospital, Army Medical University (Third Military Medical University), Chongqing, China. E-mail: 13638356728@163.com; oceanyx@126.com*

[b]*Chongqing Institute of New Energy Storage Materials and Equipment, Chongqing, China*

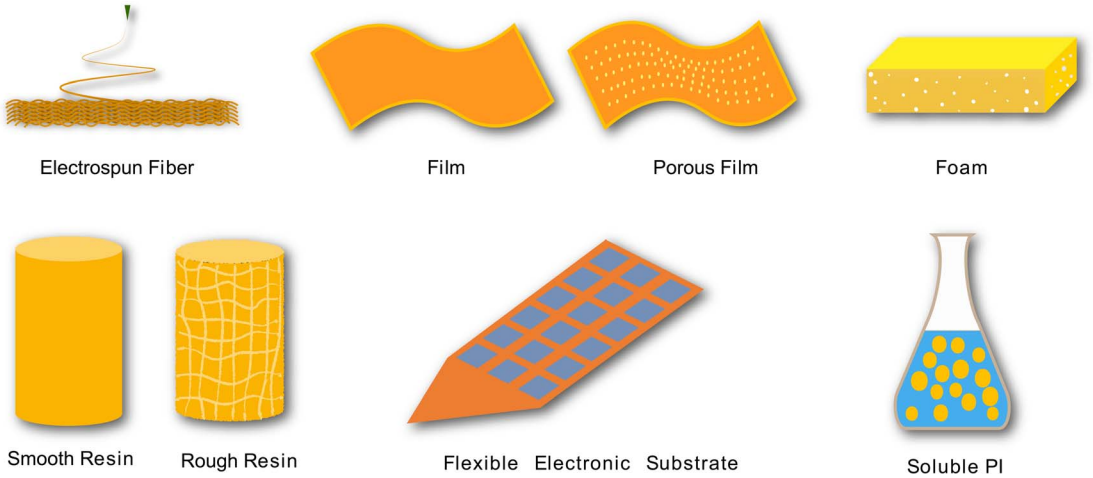

Fig. 1 Different forms of PI for different applications. PIs can be prepared as fibers, films, foams, resins, electronic substrates, and liquids for different applications.

innovate with the existing medical materials and technologies such that the materials become increasingly complicated and diversified; the performance of these newer medical materials can satisfy the demands with no additional adverse reactions.

Notably, numerous studies have shown that polyimides (PI) have excellent physical and chemical properties, including low weight, flame retardancy, high-temperature resistance, low-temperature tolerance, excellent mechanical properties, chemical solvent and radiation resistance, flexibility, and good dielectric properties.[11] It has been concluded that PI are important materials for military armor, aerospace areas, radomes, liquid crystal alignments, microelectronics, solar-to-electrochemical energy storage, photocatalysis, electrocatalysis applications, *etc.*[12] PIs are now widely used as membranes for the insulation of solar cell base plates and motor slots, separation in permeation vaporization and ultrafiltration, repairing enameled wire, and as insulating fibres in high-temperature media and bulletproof and fireproof fabrics, adhesives in high-temperature structural adhesives, photoresistant color filter films, dielectric layers and protective layers in microelectronics, orientation agents in liquid crystal displays, and electro-optical materials in optical switch fields and composites in the aviation and aerospace fields.[13,14] Additionally, advanced healthcare applications of PIs include puncture needle-type devices, artificial hip joints, microelectrode arrays for nerve stimulation,[15] drug delivery,[16,17] biosensors,[18] and other aspects of medical utilization.[19,20] Therefore, several recent studies have described the design of PIs for medical applications, including resins, powders, films, fibers, foams, and soluble PIs (Fig. 1). We aim to review the relevant literature on the synthesis, structural characteristics, properties, and application of PI as medical materials and their trends and outlook in this article.

2. Synthesis of PI

PIs with cyclic aliphatic, hetero, chiral, fluorinated, carbazole, nonlinear optical, nanometer-sized and unsymmetrical structures are derived from noncoplanar monomers (kink, spiro, and cardo structures). PIs can be divided into aliphatic and aromatic polyimides according to their chemical composition. Aromatic PIs are commonly synthesized by the polycondensation of various monomers, including diamines and dianhydrides, which are composed of a sequence of aromatic groups with imide linkages (–CO–N–CO–).[21] PI fibers were initially reported by Americans as early as the 1960s and then investigated by Japanese, Soviet, French, Austrian, and Chinese researchers.[22]

2.1 The typical PI synthesis process

The typical synthesis process of PI involves the loading of crystalline benzoic acid (BA) (9.0 g) and phthalic anhydride (PA) (0.7287 g) in a glass reactor equipped with a heater, stirrer, and an inert gas inlet. With the gas in the reactor at 140 °C, 3,4′-ODA (0.2803 g) is added to the mixture. The reaction mixture is stirred at 150 °C for 2 h, accompanied by the slow inflow of the inert gas. Then, this hot liquid reaction mixture is transferred to a glass container and cooled to room temperature. Next, the solidified reaction mixture is extracted and washed repeatedly with acetone or diethyl ether to remove excess BA. Finally, the reaction product of the polymer is filtered and dried under a vacuum, and the PI powder is obtained. An improved method reported that PI can also be obtained with 99% yield within 1 h from a polyamic acid intermediate using the beat and heat method, which includes solvent-free vibrational ball milling and a thermal treatment step.[23] After the PI powder is obtained, it can be hot-pressed at 300–380 °C or dissolved to obtain a 2% solution in chloroform, which can be used to form PI films (Fig. 2A).[24] This study presented a straightforward route to synthesize PI powders and films.

2.2 Dry- and wet-spinning methods

Studies have reported that PI fibers are mostly synthesized by dry-spinning and wet-spinning methods. In the wet-spinning

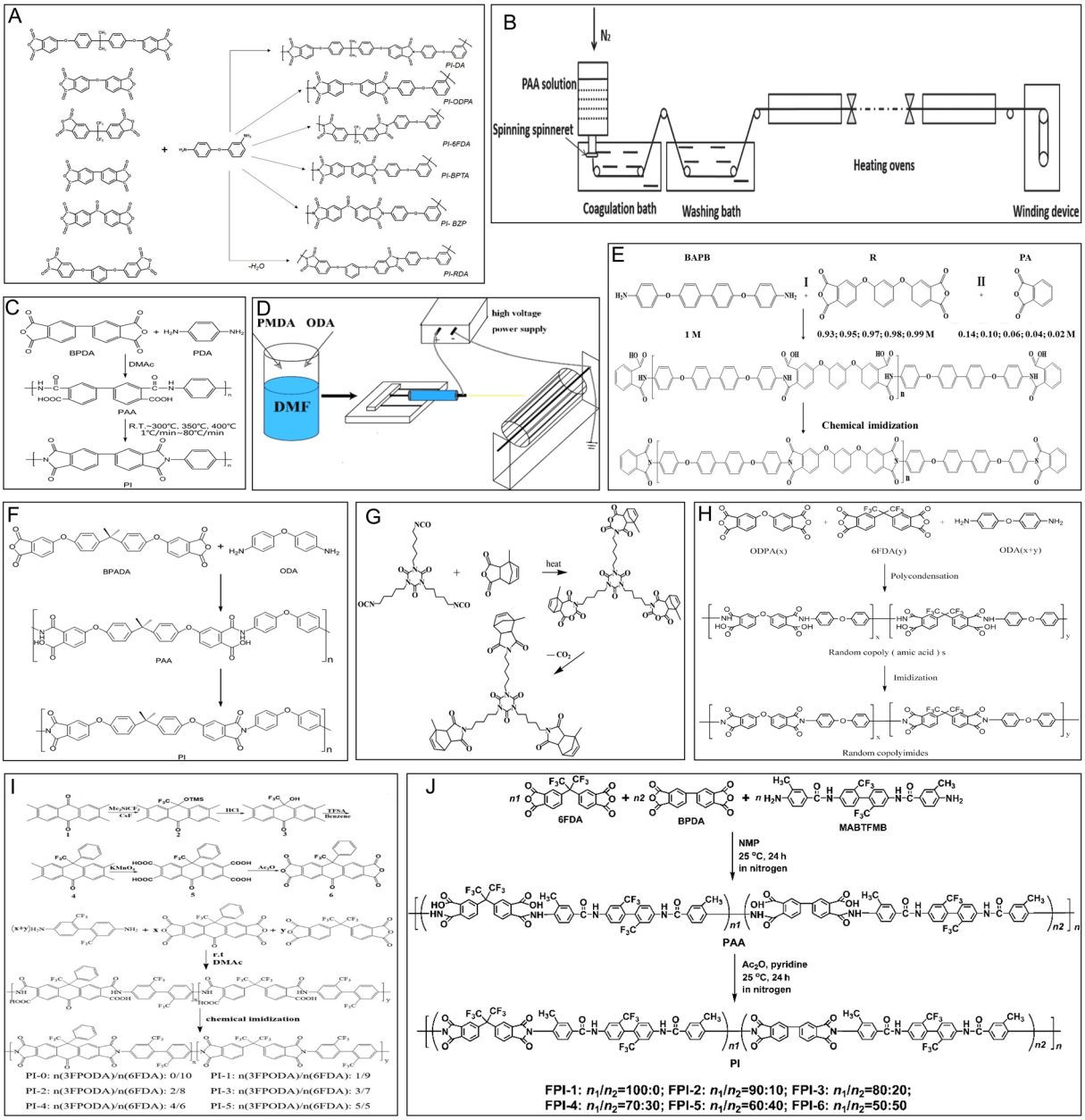

Fig. 2 Schematic representation of the synthesis of PI. (A) Synthesis of aromatic polyimides based on unsymmetrical diamine 3,4′-ODA and various tetracarboxylic acid dianhydrides. Reproduced with permission.[24] Copyright 2022, MDPI. (B) Preparation of HSHMPI fibers using an integrated continuous wet-spinning method. Reproduced with permission.[22] Copyright 2018, WILEY-VCH. (C) Synthesis of a BPDA–PDA polyimide. Reproduced with permission.[25] Copyright 2020, MDPI. (D) The electrospinning process. Reproduced with permission.[26] Copyright 2022, MDPI. (E) Synthesis of polyimide R-BAPBs with different molecular weights. Reproduced with permission.[27] Copyright 2023, MDPI. (F) Synthesis of a BPADA–ODA–PI. Reproduced with permission.[28] Copyright 2015, Nature Publishing Group. (G) Synthesis of the bismaleimide resin modified with hyperbranched polyimide. Reproduced with permission.[29] Copyright 2022, MDPI. (H) Synthesis of a 6FDA/ODPA–ODA polyimide. Reproduced with permission.[30] Copyright 2021, MDPI. (I) The preparation of 3FPODA and the synthesis of copolymerized polyimide. Reproduced with permission.[31] Copyright 2022, MDPI. (J) Synthesis of an organosoluble fluoro-containing polyimide. Reproduced with permission.[32] Copyright 2022, MDPI.

method, organic-soluble PI or polyamic acid (PAA) solutions are forced into a nonsolvent fluid to separate the fibres from the solvent. Then, the generated fibers are annealed under tension to remold the tensile strength and modulus. In contrast to the wet-spinning method, organic solvents are evaporated directly from extruded PAA fibers at high temperatures, and a partial imidization reaction occurs in a mixture of hot gases during the dry-spinning process (Fig. 2B).[22] The spinning speed is increased to improve the production of PI fibers by the dry-spinning process. The quality of PI fibers is better when using wet-spinning or dry-wet-spinning methods.

2.3 One-step and two-step processes

In addition, according to the differences in the spinning solutions and reaction mechanisms, two main strategies defined as one-step and two-step processes are used to prepare PI fibers. In a one-step method, PI fibers are produced directly from organic-soluble PI solutions boiling at 180–220 °C *via* a rapid imidization reaction. In the two-step method, PAA solutions are obtained first after reacting dianhydride and diamine monomers in dipolar aprotic solvents and then converted into the final PI fibers through thermal or chemical imidization (Fig. 2C).[25] For instance, *p*-phenylenediamine (PDA) and 3,3′,4,4′-biphenyltetracarboxylic dianhydride (BPDA) were combined to obtain the precursor fibers of PAA *via* a dry-jet wet-spinning process. Subsequently, the PAA fibers were heated from room temperature to 300, 350, and 400 °C to form PI fibers, and the tensile modulus of the PI fibers was highly dependent on the heating rate.[25] In addition, PAA has also been obtained from the reaction of 4,4′-oxydianiline (4,4′-ODA) (3.97 g) and pyromellitic dianhydride (PMDA) (4.33 g) in 35 mL of *N*,*N*-dimethylformamide (DMF) by polycondensation under stirring for 8 h. The PAA solution was electrospun at 15 kV by maintaining a distance of 15 cm from the needle to the collector and then subjected to thermal imidization (Fig. 2D).[26] Finally, PI nanofibers were obtained.

2.4 Thermoplastic or thermosetting methods

According to the processing characteristics, PI fibers can also be classified as thermoplastic or thermosetting PI. Typically, the thermoplastic partially crystalline PI powder is distributed on continuous carbon fibers *via* electrostatic spraying, and further hot calendering and pressing affords thermoplastic PI. The obtained carbon plastics show a rise in the glass transition and thermal decomposition temperatures up to 590 °C when composited with PI (Fig. 2E).[27] The physical properties of thermosetting PI include a higher glass transition temperature and storage modulus and better shape fixity than thermoplastic PI due to low-density covalent crosslinking (Fig. 2F).[28] Hyperbranched PI has also been prepared to modify bismaleimide (BMI) resin to achieve higher impact strength (Fig. 2G).[29] Based on the use of chemical or physical crosslinking reactions, thermoplastic or thermosetting processes are chosen.

2.5 The modified synthesis process

Moreover, some studies have investigated the imidization process, evaporation, chain orientation, crystallization, subprocesses of solvents, chemical conversion, and composition toward improving the properties of PI materials.[25] The PIs synthesized from symmetric 4,4′-oxydianiline (4,4′-ODA) are amorphous and have a low glass-transition temperature (Fig. 2H).[30] The introduction of 2,4,5,7-tetraamino-1,8-dihydroxyanthracene-9,10-dione (4NADA) monomers in the polyimide chains can enhance the rigidity of the structure.[33]

A new dianhydride, namely 10-oxo-9-phenyl-9-(trifluoromethyl)-9,10-dihydroanthracene-2,3,6,7-tetraacid dianhydride (3FPODA), has proven to be an ideal monomer candidate for enhancing the adhesive properties and glass transition temperatures (T_g) of colorless PI (Fig. 2I).[31] A special flexible PI film obtained using a multicomponent copolymerization methodology using the fluoro-containing dianhydride 4,4′-(hexafluoroisopropylidene)diphthalic anhydride (6FDA), the rigid 3,3′,4,4′-biphenyltetracarboxylic dianhydride (BPDA), and a fluoro-containing diamine, namely 2,2′-bis(trifluoromethyl)-4,4′-bis[4-(4-amino-3-methyl)benzamide] biphenyl (MABTFMB), showed good optical properties and excellent thermal properties (Fig. 2J).[32]

It can be concluded that the methods of PI synthesis are very complicated. By changing the elements, the ratio of monomers, and the preparation method, a great variety of PIs with different characteristics can be obtained.

The application and popularization of PI can be improved by improvements in synthesis strategies and spinning technology.

3. Properties of PIs as biological/medical materials

To be considered a biomedical material, a polymer must possess some basic characteristics. These include but are not limited to the following: the material should (1) be chemically inert and not react with body fluids; (2) not cause inflammation or foreign body reactions in human tissues; (3) not cause cancer; (4) not cause thrombosis; (5) be suitable for long-term implantation in the body, without a decrease in mechanical strength; (6) be able to withstand the necessary cleaning and disinfection measures without degeneration; and (7) be easy to process into the required complex shape. It is worth mentioning that PI not only meets all the conditions of interest but also shows beneficial biological activity.[34,35] Some of the advantageous characteristics of PI used in the medical field are discussed below.

3.1 Long-term stability

PI and PI matrix nanocomposites have attracted increasing attention in material applications due to their high thermal stability at high temperatures. The thermogravimetric degradation profiles of pure PI show that the initial decomposition of PI occurs in the temperature range of 200–400 °C because of the release of chemically bound water and evaporation of the solvent. In a relevant report, the PI matrix achieved 40% mass loss at 500–630 °C (Fig. 3A).[36] The high-temperature resistance of the PI composite films has been reportedly modified by integration with mica nanosheets (Fig. 3B).[37] In a 20 month *in vitro* study, three commercially available PIs, namely U-Varnish-S (UBE, Japan), Durimide 7510 (FUJIFILM, Japan), and PI2611 (HD MicroSystems, USA), were immersed in phosphate-buffered saline (PBS, pH = 7.4) at specific temperatures. After 20 months, the experimental PI did not undergo mass loss at 37 °C (normal human body temperature) or 60 °C (upper limit temperature for accelerated lifetime testing) in PBS, and the fracture mechanical properties, such as fracture energy, did not change (Fig. 3C–E).[38] In another work, a new thin-film PI-based electrode array was stimulated by electricity and then immersed

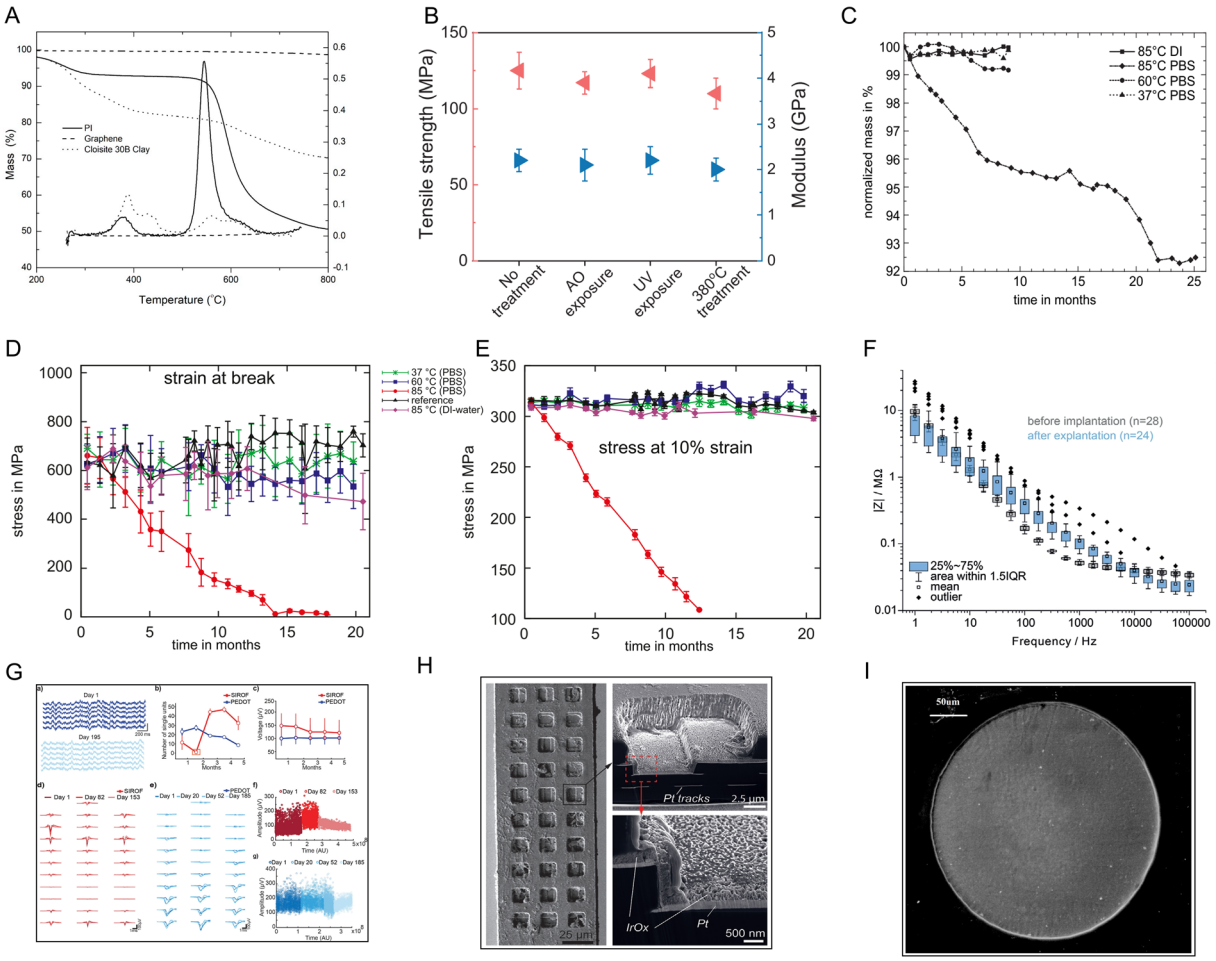

Fig. 3 Stability tests for PI. (A) TGA thermograms of neat polyimide, graphene, and Cloisite 30B clay in a nitrogen atmosphere at a heating rate of 30 °C min^{-1}. Reproduced with permission.[36] Copyright 2021, MDPI. (B) The tensile strength and Young's modulus of a PI–mica film change a little after AO, UV, and high-temperature exposure. Reproduced with permission.[37] Copyright 2013, WILEY-VCH. (C) The mass loss curve and (D and E) stress–strain curve of PI stored in PBS show that PI was stable in PBS at body temperature and even at 60 °C. Reproduced with permission.[38] Copyright 2010, Elsevier. (F) Electrochemical impedance spectra and (G) long-term imaging of a PI probe implanted in the mouse cortex for 180 d. (H) SEM image showing the overall intact probe with any signs of delamination or corrosion. Reproduced with permission.[40] Copyright 2023, WILEY-VCH. (I) SEM image of a microelectrode six months after its implantation in rabbit eyes shows no damage of the surface or accumulation of tissue matter. Reproduced with permission.[15] Copyright 2013, Springer Nature.

in PBS at body temperature (37 ± 3 °C) for 29 d. The electrical characteristics were evaluated by cyclic voltammetry (CV), electrochemical impedance spectroscopy (EIS), and voltage transients (VT). The results showed the stability of the PI electrode array.[39] PBS obviously does not fully represent the complex environment in the body. Studies on the long-term biological stability of PI *in vivo* have also been reported. After implantation in animals, the PI electrodes could work stably for months or even a year.[40–42] Cross-sectional imaging using focused ion beam scanning electron microscopy (FIB-SEM) revealed well-adhered layers of the metallic electrode and PI, and no aging phenomena, such as delamination or cracking, were observed (Fig. 3F–H).[40] Similar results were obtained after implantation of the PI material in rabbit eyes for 6 months. Light microscopy and SEM revealed that the PI materials did not obviously degrade (Fig. 3I).[15] These results suggest that PI can be an ideal implant material that maintains the dual stability of the PI itself and the implant environment.

3.2 Multiple construction processes

PI can be formulated in various forms, such as films, fibers, resins, foams, flexible electronic substrates, gas separation membranes, proton exchange membranes, and soluble PI, with different physical and chemical properties. The different forms of PI can be further modified to obtain a wide range of properties through different synthesis and processing methods, which enable great potential for PI to be designed and manufactured with variable functionalities according to different requirements. For example, stiff forms of PI can be made into puncture needle-type devices (*e.g.*, transverse intrafascicular multichannel electrodes),[43] while neural electrodes attached to the cerebral cortex require flexible PI.[44] Different curing temperatures[45] and surface modifications[46] can change the hydrophobicity and roughness of PI materials. A smooth surface is suitable for the cardiovascular system and helps reduce the risk of thrombosis,[47] while a rough surface facilitates

fibroblast and osteoblast attachment.[48] Changes in surface morphology have also been shown to strengthen the differentiation of mesenchymal stem cells into adipogenic and osteogenic lineages *in vitro*,[49] which can be applied in the field of wound repair. In addition, porous PIs can be used as drug delivery systems. Different drugs can be loaded, and the release rate can be controlled by the different pore sizes of PI.[50] Excitingly, the features of multiple construction processes of PI provide numerous chemical modifications that can be advanced to overcome the shortcomings of the currently available materials.

3.3 Biocompatibility

Material scientists recognize that biocompatibility is a characteristic of the material-biological-host response system and not the property of the material itself in a specific application.[51] Cytotoxicity testing is an essential aspect of evaluating biocompatibility. Richardson *et al.* showed for the first time that PI has no cytotoxic effects on mouse fibroblast (Swiss-3T3) cells, similar to polytetrafluoroethylene (PTFE) and polydimethylsiloxane (PDMSO) (commonly used hydrophobic substrates for plaster drugs).[52] After that, the cytotoxicity of PI toward L929 mouse fibroblasts,[53] human retinal pigment cells (Fig. 4A),[15] human epithelial cells (adherent HeLa),[54] human cerebromicrovascular endothelial cells (hCMECs) (Fig. 4B)[55] and human dermal fibroblasts[56] has been tested. Some of these studies claim to follow ISO standards strictly. Other studies have used 3-(4,5-dimethylthiazol-2-yl)-3,5-diphenyltetrazoliumbromide (MTT) assays, lactic dehydrogenase-based toxicology assays, calcein-AM, and ethidium bromide-based live/dead assays. All *in vitro* experiments suggest that PI has low/noncytotoxic effects.

Although investigators widely use cytotoxicity testing, which is the only biocompatibility experiment in many biomaterial-related studies, it is obvious that *in vitro* studies of single cell lines and simple environments are far from depicting the biocompatibility problems that occur *in vivo*. As the understanding of biocompatibility has deepened, an increasing number of studies have begun to explore hemocompatibility (*i.e.*, inability to cause hemolysis or coagulation) of PIs (Fig. 4C and D),[57] genotoxicity,[60] irritation,[61] and host response.[62] Further, thin-film PI electrodes have also been tested for biocompatibility features, including acute systemic toxicity, irritation, pyrogenicity, sensitization, immune system response, and a prolonged 28 d subdural implant *in vivo* (Fig. 4E).[58] In these studies, neither the PI nor implants with the PI, which served as the main material, were found to cause severe negative effects *in vitro* or *in vivo*. Fortunately, new thin-film PI electrodes were permitted by the US FDA for clinical trials [510(k) K192764], making them the first subdural electrodes to advance

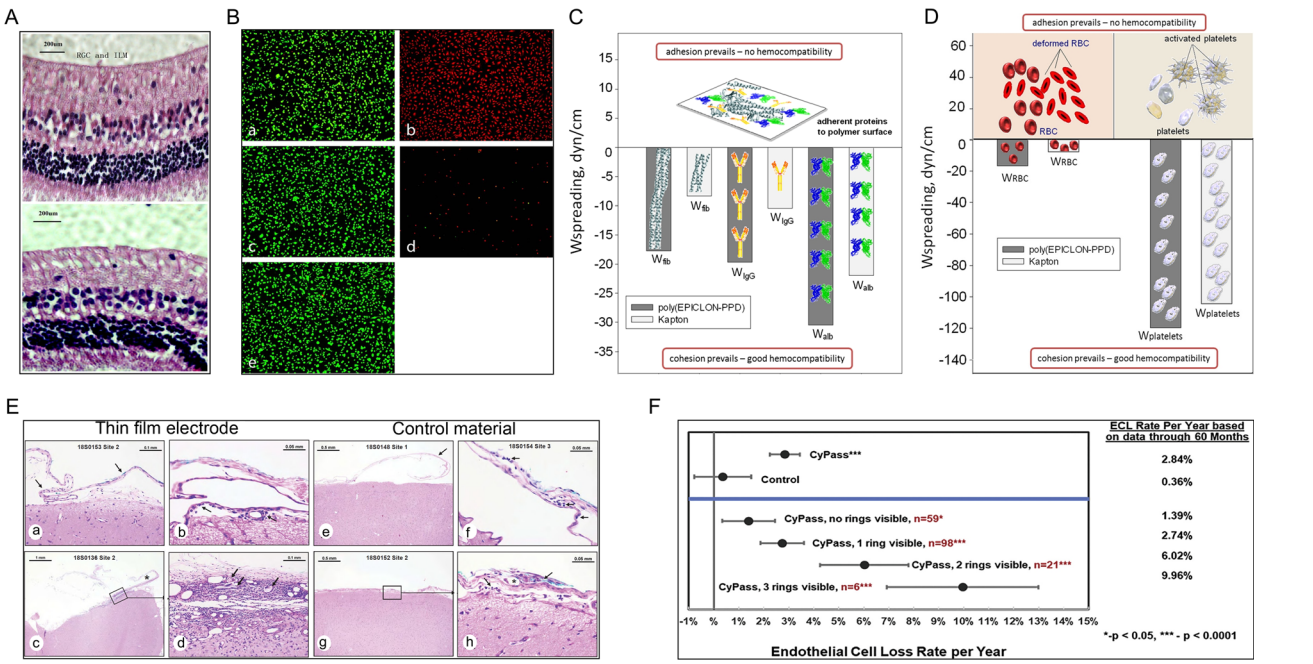

Fig. 4 Biocompatibility tests for PI. (A) Rabbit retina layer six months after PI electrode implantation (top) and control retina implantation (bottom). Reproduced with permission.[15] Copyright 2013, Springer Nature. (B) Microscopy images of endothelial cells subjected to direct contact cytotoxicity assay. (a) Untreated control. (b) Methanol-treated positive control. (c) HDPE, negative material control. (d) Latex, positive material control. (e) PI. Reproduced with permission.[55] Copyright 2013, WILEY-VCH. (C and D) Hemocompatibility tests. The spreading of (C) blood proteins, (D) red blood cells, and platelets over the surface of poly(EPICLON-PPD) and Kapton (PI) films. Reproduced with permission.[57] Copyright 2016, Springer Nature. (E) The immune responses to (a–d) a PI electrode implanted for 28 days in sheep brain were minimal compared with the response to (e–h) the negative control material. These effects were evaluated based on the accumulation of immune system cells, necrosis, neovascularization, fibrosis, and astrocytosis/fatty infiltration. Reproduced with permission.[58] Copyright 2022, Aura Kullmann. (F) Long-term safety study. PI material (CyPass) implantation increases endothelial cell loss over time in patients with cataracts. Reproduced with permission.[59] Copyright 2019, Elsevier.

rapidly from laboratory studies to clinical practice and indicating the need for more long-term *in vivo* studies of PI to prove their biocompatibility. However, a five year safety study of minimally invasive glaucoma surgery showed that patients implanted with PI materials (Micro-Stent) experienced more endothelial cell loss over time than patients who underwent the standard cataract surgery (loss of 20.4% *vs.* 10.1%) (Fig. 4F).[59] This suggests that more long-term *in vivo* studies of PI need to be performed based on special PI materials with low cytotoxicity.

4. Medical applications of polyimides

As PIs form a class of high-performance polymers, an increasing number of studies have focused on broadening the applications of PI.

The superior high- or low-temperature tolerance, resistance to chemical solvents and radiation, flexibility, dielectric properties, biocompatibility, long-term stability and multiple construction processes of PI have enabled the transition of their application from industry to medicine. The medical applications of PIs are listed and summarized in Table 1.

4.1 PI electrodes in the nervous system

Electrodes that function as signal collectors and transmitters are mainly used in the study, diagnosis, and treatment of diseases. They have attracted attention as important components of neuron–computer interfaces in recent years. For example, intracranial nerve electrodes collect raw physiological signals and are the most important part of the entire signal-processing process.[93] The integrated electrode itself must be long-lasting and stable with minimal adverse effects on the organism to collect the clearest and most stable signal (Fig. 5A).[40] The choice of substrate material is crucial. In this regard, the combination of two properties, namely flexibility and small cross-sectional area, seems to be particularly effective.[42,94] PI is an excellent material that can meet this requirement and has high potential to serve as an electrode in neural applications due to its biocompatibility,[94] electrochemical inertness,[42] electrical conductivity, and long-term stability (Fig. 5B).[40] An increasing number of studies have investigated PIs with different backbones for application in integrated microelectrodes (Fig. 5C).[42]

Microelectrodes fabricated from fully aromatic PIs show superior performance in the electrochemical monitoring of dopamine and provide evidence for the early diagnosis of neurological disorders.[63] A flexible PI has also been used as a substrate to develop epidural electrocorticography electrodes, which can monitor various neurodegenerative diseases.[64] One PI-based flexible electrode has been shown to record electrocorticography signals in multiple regions with minimal invasion of the brain (Fig. 5D).[65] Moreover, a brain intracranial electroencephalogram microdisplay engineered using a PI substrate to measure brain neuronal activity has successfully been able to identify the boundaries of normal *versus* pathological brain regions and display near-real-time changes on the surface of the brain for surgical assistance.[67] A nanofabricated PI-based microelectrode used in high-resolution mouse electroencephalography is a competent tool for recording large-scale brain activity as it exhibits the ability to distinguish the neural correlates of certain brain waves in conjunction with special behavior.[66] One special electrode that combines PI with prototype carbon could record the signaling of the neural local field with an equal or better signal-to-noise ratio and almost

Table 1 Summary of the medical applications of PI

Applications	Devices	Functions
Neural electrodes	Electrocorticography (ECoG) arrays	Dopamine monitoring,[63] high-performance neural recordings,[58,64–66] identification of pathological brain regions,[67] chronic stimulation[68]
	Peripheral electrodes	Epiretinal stimulation,[15] motor nerve stimulation,[43] denervated muscles stimulation,[69] afferent nerve simulation[70]
	Depth probes	Brain–computer interface,[40] chronic stimulation and monitoring[42]
Biosensor	Vessel-related sensors	Aneurysm monitoring,[71] stenosis monitoring,[72] extravasation detection[73]
	In vitro sensors	Electrical cell signal sensing,[74] electrochemical detection[75]
	Implant sensors	Intradiscal pressure measurement,[76] dental implant detection[77]
Drug delivery systems	PI tubes	Controlled subcutaneous drug release,[78] inner ear drug delivery,[79] intracranial drug delivery[80]
	Microneedles	Painless subcutaneous drug delivery[81,82]
	Transdermal patches	Electrothermal and photothermal triggered drug release[83,84]
	PI-COF	High drug loading and well-controlled release[50]
Tissue replacements	Artificial bones	Osteogenesis and osseointegration induction[85–87]
	Artificial muscle	Simulation of perimysial collagen fibers[88]
Respirators	Medical masks	Self-friction-induced electric energy generation,[89] photothermal self-purification[90]
Antibacterial material	Medical catheter	Anti-biofilm formation,[91]
	Anticoagulant membrane	Antibacterial adhesion[92]
	Dressing	Bacteria killing and healing promotion[34]

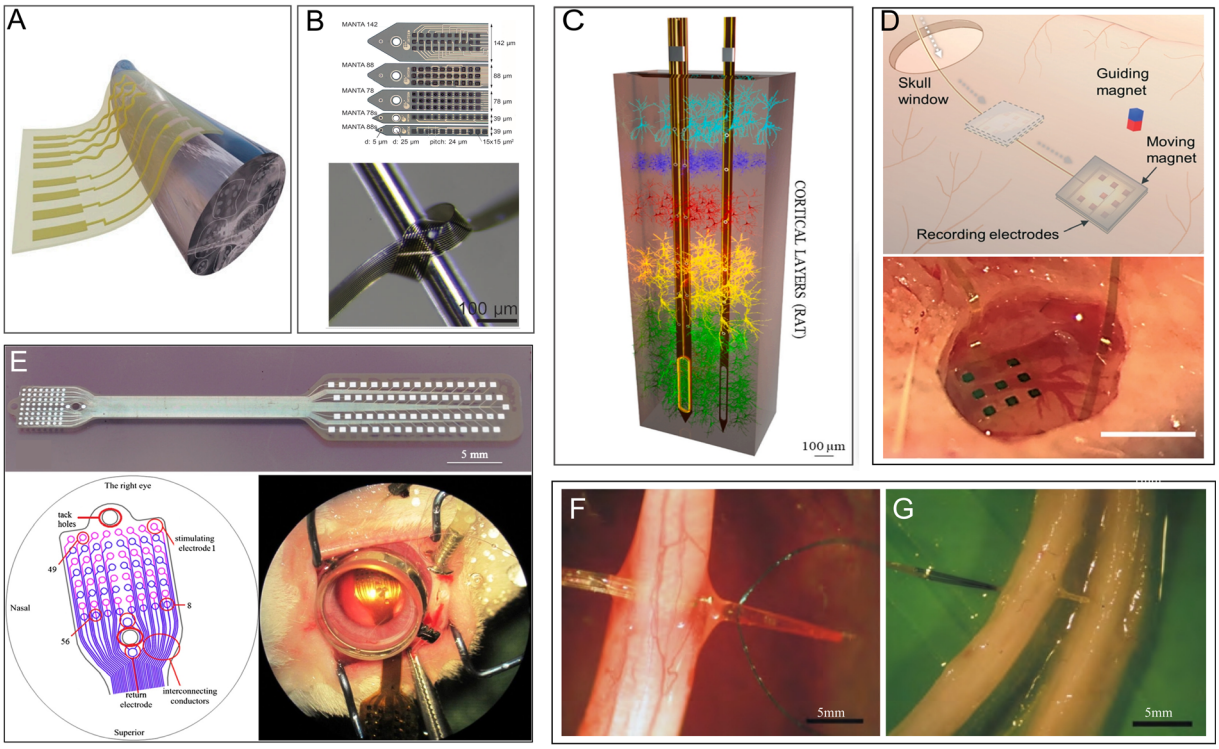

Fig. 5 PI electrodes in the nervous system. (A) Schematic illustration of flexible nanomembranes wrapped around a sciatic nerve for long-term application of electrical stimuli and sensing. Reproduced with permission.[95] Copyright 2022, PNAS. (B) Thin-film intracortical multilayer array probe, which is robust and flexible. Reproduced with permission.[40] Copyright 2023, WILEY-VCH. (C) 3D representation of the depth of probes within the brain cortex of a rat. Reproduced with permission.[42] Copyright 2022, Elsevier. (D) Subdural electrocorticography (ECoG) electrode arrays positioned in the rat brain through a small window in the skull. Reproduced with permission.[65] Copyright 2021, the Royal Society of Chemistry. (E) A stimulating thin-film microelectrode array implanted on the surface of rabbit retina. Reproduced with permission.[15] Copyright 2013, Springer Nature. (F and G) A transverse intrafascicular multichannel electrode (TIME) device transversally implanted though (F) the rat sciatic nerve and (G) the median human nerve. Reproduced with permission.[43] Copyright 2010, Elsevier.

completely remove image artifacts at magnetic fields of strength up to 9.4 T; thus, it is potentially useful in electrophysiology and magnetic resonance imaging for neurological diseases.[96] In addition, PI electrodes are also applied in the robotic arms of amputees for recording output signals from human nerves.[70] Photosensitive PI microelectrode arrays (epiretinal bio-MEAs) implanted in the visual cortex of rabbit eyes successfully record the response to electrical stimuli (Fig. 5E).[15]

Furthermore, electrical neuron stimulation is a promising method for treating and diagnosing chronic neurological diseases, such as epilepsy. New thin-film PI electrodes have been authorized for use in clinical trials for the surgical evaluation of patients with drug-resistant epilepsy by the FDA.[58] In a relevant study, a microlight-emitting diode array with a flexible PI film as a chronic photostimulation unit and a whole-cortex electrocorticographic electrode as a recording unit were implanted into the cerebral cortex of common marmosets for 4 months. This device gradually increased neural responses after photostimulation for ~8 weeks[68] and shows potential for application in epilepsy treatment. In peripheral nerves, PI-based implantable flexible microelectrode arrays (MEAs), which provide nerve stimulation and recording, implanted on the surface of long-term denervated muscles have been shown to reduce the atrophy of the denervated muscle while retaining more acetylcholine receptors.[69] In another work, a transverse intrafascicular multichannel electrode was transversally implanted into the rat sciatic nerve and the median human nerve to interface with the peripheral nerve (Fig. 5F and G).[43] PI-based MEAs have been further used for the stimulation of the remaining retinal neurons in patients with degenerated photoreceptors.[15,97]

However, mice implanted with PI-based microelectrodes on free muscle flap grafts and subjected to electrical stimulation for 6 weeks exhibited an increased inflammatory response, myopathy, and partial necrosis.[98] These studies suggest that the multiple functionalities of PI electrodes provide exciting opportunities for fundamental neuroscience studies, as well as stimulation-based neural therapies, but future work should be carefully designed to investigate the optimal electrode material, graft, and stimulated phase.

4.2 PI in biosensors

Implantable or noninvasive biosensors used as real-time monitors are powerful devices for the diagnosis and prediction of diseases and maintenance of human health as they can monitor and provide continuous or regular biometric signals. Like neural electrodes, biosensors (which transmit physical or

chemical signals) often use PI as the sensor substrate because of its good biocompatibility, hemocompatibility, and other properties. Thin, flexible, and implantable PI neuroprobes are employed in aptamer-field-effect transistor biosensors for neurochemical signaling monitoring.[18] PI has also been applied in interventional procedures, such as real-time monitoring of cerebral aneurysm hemodynamics (Fig. 6A).[71] The microphone array integrated into the PI can be used to qualify hemodialysis vascular access dysfunction (location and degree of stenosis) (Fig. 6B).[72] A novel biosensor manufactured using an array of 64 hybrid cantilevers with a PI substrate could detect adverse drug-induced effects at early stages, such as depolarization and *torsade de pointes*, in cardiomyocytes (Fig. 6C).[16] A miniature fiber optic pressure sensor fabricated with PI, which is tiny enough to be implanted into rodent discs without changing the structure or changing the intradiscal pressure, has been first successfully applied for intradiscal pressure measurements in rodents (Fig. 6D).[76] Furthermore, a multichannel temperature sensor fabricated using a flexible PI film could be wrapped around a dental implant abutment wing to send real-time warning signals before failure of the implant (Fig. 6E).[79]

It has also been reported that biosensors made with PI as a substrate have excellent abilities for trace-level or specific detection of some hormones, glucose, and gases produced by the body or others. For instance, a flexible biosensor prepared by the direct synthesis of molybdenum disulphide (MoS_2) on a PI substrate could sensitively determine endocrinopathy by measuring endocrine-related hormones, such as parathyroid hormone (PTH), triiodothyronine (T3), and thyroxine (T4), in clinical patient sera.[101] Ultrasensitive sensor arrays on PI substrates can be used for multiplexed and simultaneous electrochemical detection of cardiac damage markers, cardiac troponin-I (cTnI) and cardiac troponin-T (cTnT), in human serum.[102] A porous PI film sensor combined with grafted MgO-templated carbon has been applied to sensitively measure acetaldehyde gas released by the human skin, even at low concentrations.[103] Similarly, a special human sweat-based wearable glucose sensor microfabricated with reduced graphene oxide on

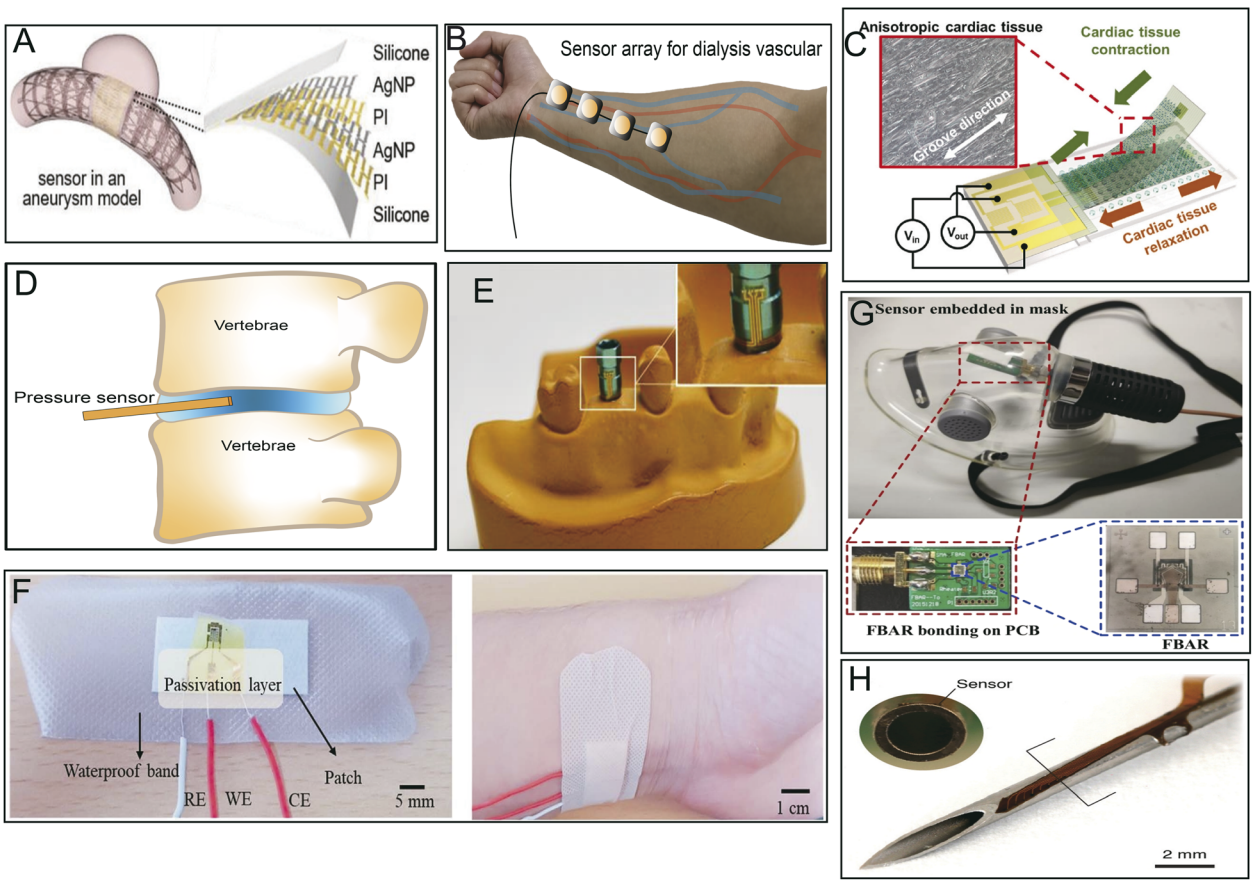

Fig. 6 Different applications of PI-based biosensors. (A) Implantable batteryless biosensor for real-time monitoring of cerebral aneurysm hemodynamics. Reproduced with permission.[71] Copyright 2019, WILEY-VCH. (B) Flexible sensor array for dialysis vascular access monitoring (recording and processing of blood flow sounds to determine stenosis risk).[72] (C) Integrated strain sensing platform for high-throughput drug toxicity screening. Reproduced with permission.[16] Copyright 2021, Elsevier. (D) Miniature pressure sensor for intradiscal pressure measurements. Reproduced with permission.[76] (E) A temperature sensor adhered around an abutment wing of the dental implant platform. Reproduced with permission.[77] Copyright 2020, MDPI. (F) Wearable sweat-based glucose biosensor. Reproduced with permission.[99] Copyright 2018, Elsevier. (G) Film bulk acoustic resonator humidity sensor. Reproduced with permission.[100] Copyright 2022, MDPI. (H) Microsensor array mounted on a 1.25 mm diameter needle for early detection of extravasation in intravenous therapy. Reproduced with permission.[73] Copyright 2022, Elsevier.

a flexible PI substrate and integrated with chitosan–glucose oxidase composites exhibited sensitive, rapid, and stable response in detecting glucose present in human sweat (Fig. 6F).[99]

A PI-based film bulk acoustic resonator (PI-FBAR) humidity sensor was utilized for the first time to detect human respiratory rates in real-time *in vitro* (Fig. 6G).[100] Likewise, a biosensor made of highly porous graphitic carbon electrodes fabricated with commercial PI tape has been shown to offer rapid, low-cost, time-saving, selective, and sensitive electrochemical detection of cytokines, such as IL6, for point-of-care analysis.[75] In addition, neuronal cells were generated on Kapton PI biosensors printed with a few layers of graphene ink to evaluate the electrophysiology and electrical signaling of Parkinson's disease *in vitro*.[74] Lin R. *et al.* reported that an ultrathin PI microsensor array can be integrated into a puncture needle for early detection of small volumes of blood extravasation (Fig. 6H).[73] Because of the small spring constant of PI, PI/Si/SiO_2-based piezoresistive microcantilever biosensors could be developed to sensitively and precisely detect aflatoxin B1 in various foods and other biomolecules.[104] Sensors integrated with PI as substrates have the potential to serve as innovative examination or analytic platforms owing to their high throughput, sensitivity, biocompatibility, and simplified data analysis.

4.3 PI in drug delivery systems

Drug modifications, microenvironmental modifications, and drug delivery systems are the three core paradigms of drug delivery technology. Drug delivery systems serve as an interface between the drug and its microenvironment, thus adjusting and optimizing the activity of the drug.[17]

PI polymers form the basis of many drug delivery systems and impart multiple functions, such as controlled release and targeted release. PI tubing with micro-holes in the tube wall and drug loaded in the lumen has been developed into a diffusion-controlled reservoir-type implantable device,[78] which when implanted subcutaneously in mice, achieved stable drug release for several months (Fig. 7A).[105] Microneedles are advanced transdermal drug delivery systems. The introduction of PI can increase the mechanical strength of microneedle arrays of carbon nanotubes, providing skin penetration with a smaller insertion force (Fig. 7B).[81,82] In interventional surgery, a cephalad-oriented PI microcatheter in the internal carotid artery has been demonstrated to allow reproducible delivery of drugs to the ipsilateral cerebral hemisphere (Fig. 7C).[80] The drugs gentamicin, dexamethasone, and lidocaine have also been delivered to the tympanic chamber using PI microtubing that passes through the round window membrane into the cochlea.[94]

A special covalent organic framework (COF) synthesized from PI loaded with ibuprofen exhibited high drug loading and well-controlled release (Fig. 7D).[50] PI-based transdermal skin patches have been applied for the controlled release of ondansetron after chemotherapy.[83] Similarly, transdermal patches made of a PI and reduced graphene oxide composite have also been used for insulin delivery (Fig. 7E).[84] Additionally, flexible PI probes have been used for highly localized drug delivery and to study electrical and chemical information exchange and communication between cells both *in vitro* and *in vivo* (Fig. 7F).[106]

PI-based drug delivery devices are a promising way to achieve precision, high-volume loading, good release control, and safety in drug delivery applications.

4.4 PI in bone tissue replacements and artificial muscles

It is universally acknowledged that metallic materials are the most commonly used implants for load-bearing bone repair.[107] However, metallic implants with a high elastic modulus have stress-shielding effects, which result in bone resorption and bone atrophy, leading to loosening or failure of the implants.[108] Due to their relative inertness, superior mechanical strength, elastic modulus, bioactivity, and biocompatibility, PI biomaterials are attractive bone tissue and joint replacement candidates

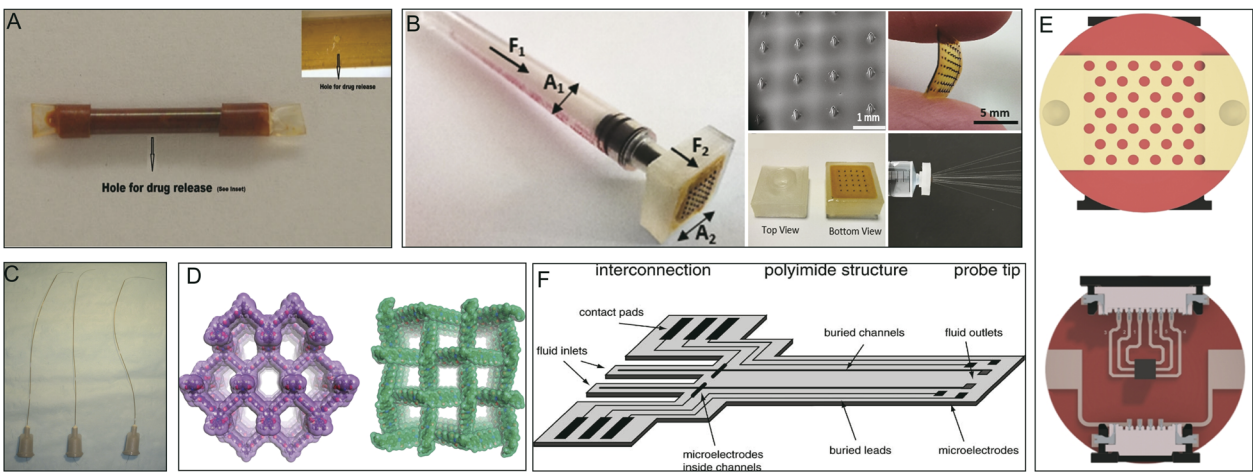

Fig. 7 PIs in drug delivery systems. (A) Perforated PI tube for subcutaneous implantation. Reproduced with permission.[105] Copyright 2012, Springer US. (B) Hollow MN array for transdermal drug delivery. Reproduced with permission.[81] Copyright 2022, Royal Society of Chemistry. (C) PI microcatheters for intra-arterial delivery. Reproduced with permission.[80] Copyright 2013, Elsevier. (D) Structural representations of 3D porous PI covalent organic frameworks. Reproduced with permission.[50] Copyright 2020, ACS. (E) Electrothermal patches with PI substrates. Reproduced with permission.[84] Copyright 2020, Royal Society of Chemistry. (F) Illustration of an implantable, flexible PI probe with microelectrodes and microfluidic channels. Reproduced with permission.[106] Copyright 2004, Elsevier.

that can replace traditional cartilage materials. The biological inertness of PI indicates a reduced inflammatory response. However, when a bioinert PI material is used as a bone substitute, it does not induce a cellular response, bone development and repair or osteointegration, which are highly important for eventual bone healing.[109]

To resolve this problem, the surface bioactive properties of PI used as potential bone substitutes have to be improved.[38] Kaewmanee *et al.* used concentrated sulfuric acid to treat PI, creating microporous surface phenotypes. At the same time, flower-like molybdenum disulphide submicron-spheres added to sulfuric acid in advance were attached to the microporous surface of PI, resulting in the final PI–molybdenum disulphide composite, which exhibited good osteogenic and antibacterial functions (Fig. 8A–F).[85] Moreover, microporous PI coated with 15 wt% tantalum oxide submicron-size particles resulted in greater bioactivity, inducing cellular responses (such as proliferation, adhesion, and alkaline phosphatase activity) in the bone marrow stromal cells of rats (Fig. 8G–L).[110] In particular, Zhang *et al.* reported that a 40 wt% nanolaponite ceramic fabricated with PI through melt processing could increase the bioactivity of PI as an implantable material for bone repair. The greater amount of apatite deposited on this composite material indicated good bioactivity; it exhibited outstanding proliferation, cell adhesion, and alkaline phosphatase activity in rat bone mesenchymal stem cells *in vitro* and remarkably induced osteogenesis and osseointegration in male beagle dogs *in vivo*.[86]

In addition, PIs are also used in the design of artificial muscles. Ling *et al.* added a corrugated grid-like PI scaffold inside a muscle prosthesis to simulate undulated perimysial collagen fibers surrounding the myocardium, rendering the contraction of the muscle prosthesis direction dependent and more in line with physiological conditions.[88]

Overall, these findings show that this bioengineering approach involving PI provides promising strategies for fabricating biomimetic bone substitutes for bone repair and muscle reconstruction.

4.5 PI in face masks or respirators

The traditional N95 mask provides 85% protection against sub-300 nm particles. Unfortunately, it cannot protect against pathogens, such as the COVID-19 virus, which have a diameter range of 65–125 nm.[111] Since the outbreak of COVID-19 across the globe, antipathogen mask design and decontamination methods involving N95/N99 masks have been preferentially studied and developed.[112] By leveraging the hydrophobicity and low pore size (down to 5 nm) of PI nanofiber membranes, investigators have focused on the outstanding filtering performance of PI materials. Masks made of PI electrospun fibers with embedded metal–organic frameworks have been shown to perform well at filtering volatile organic compounds (represented by formaldehyde).[113] Polyimide and polyethersulfone solutions have been used in electrospinning to develop nanofiber membranes with excellent particulate matter filtration efficiency, excellent nano-aerosol filtration quality, excellent interception ratios against bacteria and viruses (above 99%), and nontoxic effects on cells.[114] In addition, PI has also been employed in the design of photothermal self-purification masks. With the help of plasmonics, the surface temperature of these respirators is increased to more than 80 °C within 1 min after exposure to sunlight, enabling convenient inactivation of microorganisms and reuse.[90] However, in the study by Ghatak *et al.*, the PI–nylon composite did not show a superior triboelectric ability to latex rubber.[115] This finding suggests that the filtration efficiency of the PI mask needs to be confirmed against bacteria, viruses, volatile organic compounds, and polluted air before use. Crucially, the low price of raw materials makes the mass generation of PI-based masks feasible.

4.6 PI as an antibacterial material

The reported experimental results show that the antibacterial abilities of PI materials include antibacterial adhesion, antibacterial biofilm formation, inhibition of bacterial growth under coculture, and accelerated wound healing of infection.

It is worth noting that some studies exploring the antimicrobial effect of PI composites have only tested the antimicrobial ability of the composite as a whole and have not tested PI alone when PI is considered a hydrophobic matrix/carrier, so the antimicrobial activity may be due to the non-PI component.[85] It has also been found that PIs used in composite materials exhibit low antibacterial activity.[87,110,116] In a relevant study, PIs modified with a concentrated sulfuric acid suspension containing 15% tantalum oxide submicron-sized particles (named PIST15) exhibited improved antibacterial properties.[110] However, topographically and chemically modified commercial PI films (Kapton, American) showed improved antibacterial properties, with decreased adhesion and growth of *Pseudomonas aeruginosa* (*P. aeruginosa*) but did not trigger cell death in the attached bacteria.[117]

Recently, successful attempts have been reported using only PI to make antibacterial catheters and dressings (here, PI is not the matrix of a composite antimicrobial material). Lee *et al.* developed a surface-modified medical PI catheter that could form an antifouling layer, as its surface was modified with hydrophilic amino acids. *In vitro* experiments show that the adhesion of bacteria, fibrinogen, and albumin on the surface of the duct decreased significantly, which is highly important for the prevention of catheter-associated infections.[91] Polymer films synthesized based on 2-methacryloyloxyethyl phosphorylcholine-modified hyperbranched PI directly and significantly reduced the number of adhesive bacteria and demonstrated improved antibacterial properties in *in vitro* experiments.[92] Similarly, $CuFe_2O_4$@SiO_2–PI nanoparticles exhibited good biocompatibility with HEK293T cells and antibacterial properties against *P. aeruginosa*, *Escherichia coli* (*E. coli*), and *Staphylococcus aureus* (*S. aureus*).[118] Our group has reported wound dressings made of PI fibers with significant antimicrobial effects against methicillin-resistant *S. aureus* (MRSA) and *E. coli* in *in vitro* experiments. We found that the PI fibers directly damaged the cell walls of both bacteria. *In vivo*, these PI dressings effectively improved local infection of smeared wounds in mice, inhibited the bacterial load and

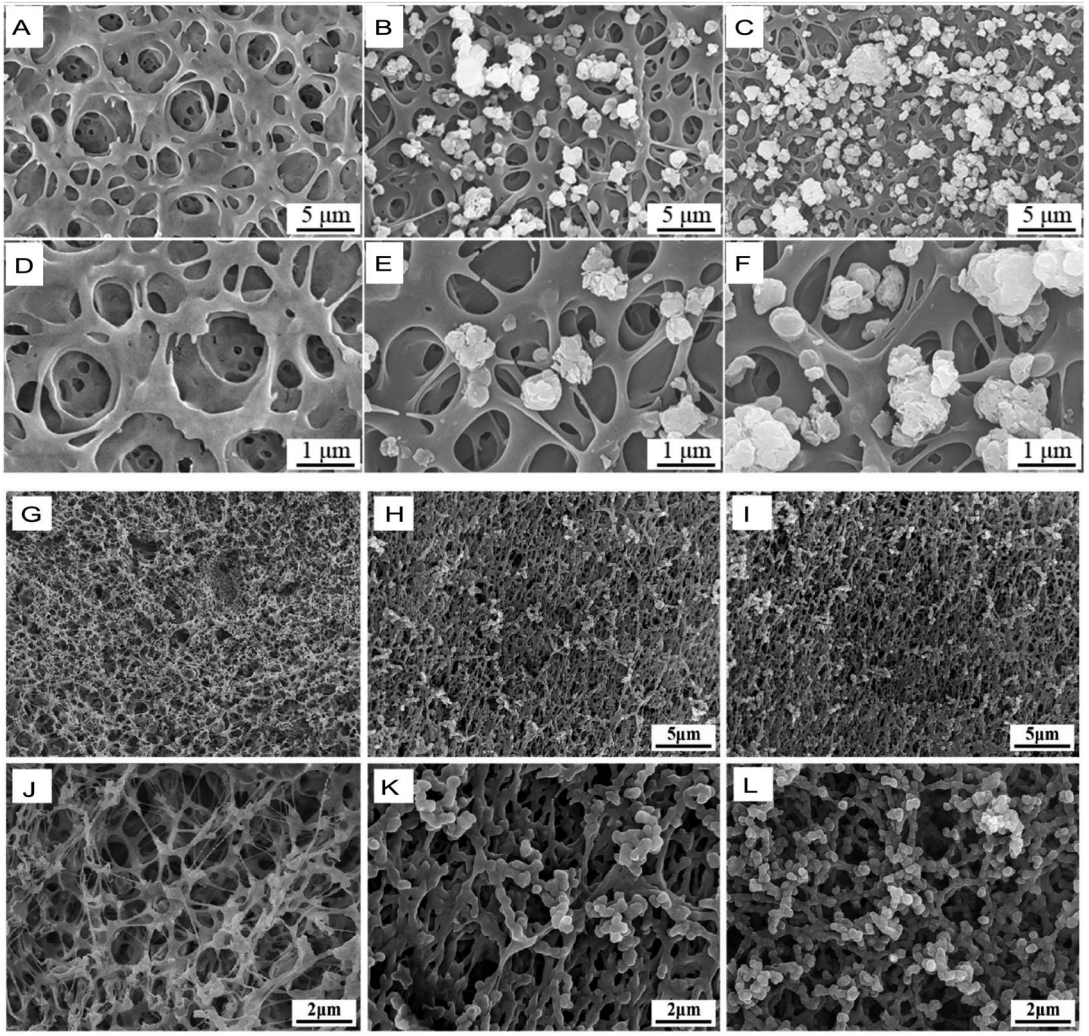

Fig. 8 SME images of different polyimide-based composites for bone replacement. (A–C) Flower-like molybdenum disulfide (fMD)–PI composites with 0%, 5 wt% and 10 wt% fMD contents. (D–F) Images in (A–C) at higher magnification. Reproduced with permission.[85] Copyright 2022, Royal Society of Chemistry. (G–I) Tantalum oxide (vTO)–PI composites (PISTs) with 0%, 10%, and 15% vTO contents. (J–L) Images in (G–I) at higher magnifications. Reproduced with permission.[110] Copyright 2021, Elsevier.

infiltrating macrophages, and accelerated the healing of pathogen-infected wounds.[34] We used other forms of PI materials with similar raw materials but different polymerization reactions to investigate the antibacterial properties of these materials (Fig. 9). However, only specific PI fibers exhibited significant antibacterial effects *in vitro*.[34]

Studies have shown that PI materials have excellent antibacterial properties and possess many other advantages, such as biocompatibility, long life, and reusability. These successful examples indicate that PI antimicrobial materials are likely to be applied in clinical practice in the near future.

5. Trends and outlook

Recent progress in controlled polymerization has led to the development of diverse and complex composites for various applications. PI is considered a kind of polymer material with the best overall performance and has been widely investigated due to its unique features and application in advanced materials. However, despite the great extent of progress summarized in this review, some challenges remain to sorted in either theoretical or practical aspects for PI technology to be translated into practical PI materials in the medical field in the future.

Methods to control the appearance, characteristics, and function of PIs for medical applications have been developed. Synthesizing composite materials and changing the inherent properties of PIs are possible ways to improve the application range of PIs. With currently available technology, it is easy to change some properties of PI, such as morphology, hardness, thermal conductivity, and insulation. However, with the rapid development of polymers for use in the medical field, both *in vitro* and *in vivo*, more PIs with better performance need to be developed. For example, improving the electrical feasibility of insulating PIs has attracted increasing attention. Conductive materials offer advantages, such as complex conductive-biomaterial-based

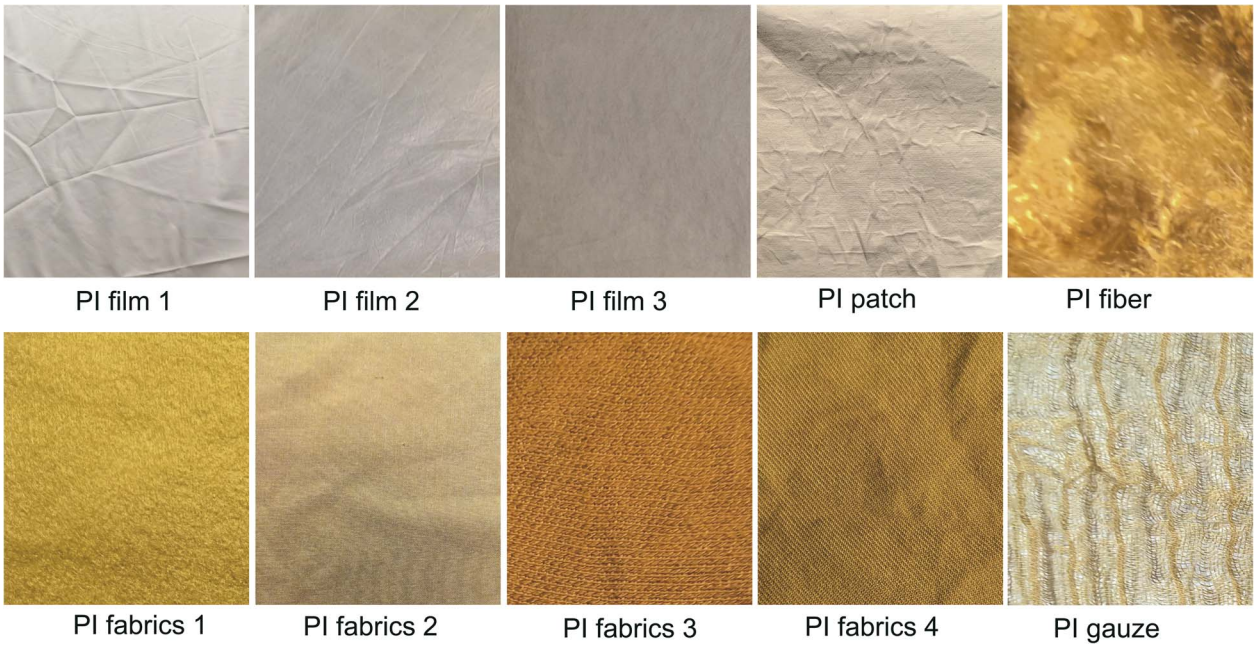

Fig. 9 Different types of PIs synthesized for the analysis of antibacterial properties. The different forms of PI tested included films, patches, fibers, fabrics, and gauze.

wound dressings with conductivity similar to that of human skin, which can significantly enhance wound healing.

As the complexity of electrodes increases, the challenges associated with their manufacture and clinical applications also increase. Overcoming the tissue damage upon electrode implantation, and the inevitable glial scarring, inflammation, and neuronal loss accompanying all implantable neurotechnologies within months remains the greatest challenge. Furthermore, to protect the functional neuronal circuitry near the electrodes, a great deal of effort has been made to improve the biocompatibility of neural probes.

In sensors, the challenges include detection at ultralow analyte concentrations (down to parts per billion or nanomolar levels), coping with complex sample matrices containing numerous interfering species, addressing issues related to differentiating isomers and structural analogs and managing intricate, multidimensional data sets. Advanced artificial intelligence techniques, including machine learning, can help boost the performance of these kinds of sensors used in medical applications, nanotoxicology, neural prostheses, wireless technology, smart agriculture, environmental monitoring, and advanced medical manufacturing technologies.

There is an urgent need for modified industrial and medical masks that can provide additional air filtration and deactivate pathogens using various technologies. In this regard, filter membranes designed based on PI fibers featuring macro, meso-, and micropores provide good filtration efficiency. Investigators are also trying to take advantage of the electrical energy generated by the self-friction of masks to directly kill pathogens or provide electricity to power sensors and antipathogenic devices.

Researchers have investigated the cytotoxicity of PI, particularly the fate of PI when it interacts with mammalian cells or when implanted *in vivo*. A good comprehension in this area will lead to the development of next-generation PI medical materials that guarantee safety in clinical applications.

6. Conclusion

The demand for biomaterials and medical devices has been on the rise recently worldwide. The safety and performance of these materials in the relevant conditions and the environment are priorities so that patients would benefit the most from organ function repair. PI is one of the most important high-performance and advanced polymers used in this field. In this review, we have discussed the chemical composition, structural features, spinning solutions, and reaction mechanism and then summarized the properties of PIs and their practical applications. Current research suggests that different forms of PI, including power, films, fibers, resins, foams, and soluble PI, have different characteristics and applications. PIs have been studied and manufactured as neural electrodes, sensors, drug delivery systems, tissue replacements, masks, antimicrobial catheters, and antimicrobial dressings in healthcare. Overall, this review presents a design guideline for future PI materials/devices and can help investigators overcome obstacles to achieve further functional improvement in PI applications in the medical field.

Conflicts of interest

There are no conflicts of interest to declare.

Acknowledgements

This research was supported by the Specialized Program (No. 2022-JCJQ-ZD-224-12) and the Chongqing Talent Project (No.

Cstc2021ycjh-bgzxm0340). We want to thank Prof. Zheng Chunfu for helpful discussions and for polishing the grammatical presentation of this manuscript.

References

1 L. De Laporte and F. Kiessling, *Adv. Healthcare Mater.*, 2023, **12**, 2301637.
2 M. Wilczynski, O. Wilczynska and W. Omulecki, *Klin. Oczna.*, 2009, **111**, 21–25.
3 Y. Wang, Y. Liu, Q. Han, H. Lin and F. Liu, *J. Membr. Sci.*, 2022, **649**, 120359.
4 D. Y. Fuhrman, E. K. Stenson, I. Alhamoud, R. Alobaidi, G. Bottari, S. Fernandez, F. Guzzi, T. Haga, A. Kaddourah, E. Marinari, T. H. Mohamed, C. J. Morgan, T. Mottes, T. M. Neumayr, N. J. Ollberding, V. Raggi, Z. Ricci, E. See, N. L. Stanski, H. Zang, E. Zangla, K. M. Gist and W.-R. Investigators, *JAMA Netw. Open*, 2024, **7**, e240243.
5 E. H. Leung, A. Gibbons and D. D. Koch, *Ophthalmology*, 2020, **127**, 859–865.
6 A. Garcia and N. D. Giraldo, *Biomedica*, 2022, **42**, 707–716.
7 A. Shariati, S. M. Hosseini, Z. Chegini, A. Seifalian and M. R. Arabestani, *Biomed. Pharmacother.*, 2023, **158**, 114184.
8 Y. Tamura and T. Abe, *Clin. Case Rep.*, 2023, **11**, e7276.
9 E. Spaziani, A. Di Filippo, P. Francioni, M. Spaziani, A. De Cesare and M. Picchio, *Acta Chir. Belg.*, 2018, **118**, 48–51.
10 L. Wang, M. Xin, M. Li, T. Zhang, Y. Pang and Y. Mao, *Carbohydr. Res.*, 2024, **538**, 109078.
11 S. Ma, S. Wang, S. Jin, Y. Wang, J. Yao, X. Zhao and C. Chen, *Polymer*, 2020, **210**, 122972.
12 Y. Zhang, Z. Huang, B. Ruan, X. Zhang, T. Jiang, N. Ma and F. C. Tsai, *Macromol. Rapid Commun.*, 2020, **41**, e2000402.
13 K. Choi, A. Droudian, R. M. Wyss, K. P. Schlichting and H. G. Park, *Sci. Adv.*, 2018, **4**, eaau0476.
14 H. S. Bi, X. X. Zhi, P. H. Wu, Y. Zhang, L. Wu, Y. Y. Tan, Y. J. Jia, J. G. Liu and X. M. Zhang, *Polymers*, 2020, **12**, 217.
15 X. Jiang, X. Sui, Y. Lu, Y. Yan, C. Zhou, L. Li, Q. Ren and X. Chai, *J. NeuroEng. Rehabil.*, 2013, **10**, 48.
16 D. S. Kim, Y. J. Jeong, A. Shanmugasundaram, N. E. Oyunbaatar, J. Park, E. S. Kim, B. K. Lee and D. W. Lee, *Biosens. Bioelectron.*, 2021, **190**, 113380.
17 A. M. Vargason, A. C. Anselmo and S. Mitragotri, *Nat. Biomed. Eng.*, 2021, **5**, 951–967.
18 C. Zhao, T. Man, Y. Cao, P. S. Weiss, H. G. Monbouquette and A. M. Andrews, *ACS Sens.*, 2022, **7**, 3644–3653.
19 X. Dong, L. Chen, J. Liu, S. Haller, Y. Wang and Y. Xia, *Sci. Adv.*, 2016, **2**, e1501038.
20 M. Kanno, H. Kawakami, S. Nagaoka and S. Kubota, *J. Biomed. Mater. Res.*, 2002, **60**, 53–60.
21 S. A. Tharakan and S. Muthusamy, *RSC Adv.*, 2021, **11**, 16645–16660.
22 M. Zhang, H. Niu and D. Wu, *Macromol. Rapid Commun.*, 2018, **39**, e1800141.
23 T. Rensch, S. Fabig, S. Gratz and L. Borchardt, *ChemSusChem*, 2022, **15**, e202101975.
24 A. E. Soldatova, R. N. Shamsutdinova, T. V. Plisko, K. S. Burts, A. Y. Tsegelskaya, D. A. Khanin, K. Z. Monakhova, T. S. Kurkin, A. V. Bildyukevich and A. A. Kuznetsov, *Materials*, 2022, **15**, 6845.
25 W. Yang, F. Liu, H. Chen, X. Dai, W. Liu, X. Qiu and X. Ji, *Polymers*, 2020, **12**, 510.
26 Z. Chang, X. Sun, Z. Liao, Q. Liu and J. Han, *Polymers*, 2022, **14**, 3230.
27 G. Vaganov, M. Simonova, M. Romasheva, A. Didenko, E. Popova, E. Ivan'kova, A. Kamalov, V. Elokhovskiy, V. Vaganov, A. Filippov and V. Yudin, *Polymers*, 2023, **15**, 2922.
28 X. Xiao, D. Kong, X. Qiu, W. Zhang, Y. Liu, S. Zhang, F. Zhang, Y. Hu and J. Leng, *Sci. Rep.*, 2015, **5**, 14137.
29 L. Yu, Y. Yu, J. Shi, X. Zhang, F. Gao, C. Li, Z. Yang and J. Zhao, *Polymers*, 2022, **14**, 4234.
30 Y. Zi, D. Pei, J. Wang, S. Qi, G. Tian and D. Wu, *Polymers*, 2021, **13**, 3222.
31 Y. Wang, X. Liu, J. Shen, J. Zhao and G. Tu, *Polymers*, 2022, **14**, 4132.
32 X. Ren, H. Wang, X. Du, H. Qi, Z. Pan, X. Wang, S. Dai, C. Yang and J. Liu, *Materials*, 2022, **15**, 6346.
33 B. Liu, Y. Zhou, L. Dong, Q. Lu and X. Xu, *iScience*, 2022, **25**, 105451.
34 X. Yang, W. Ma, H. Lin, S. Ao, H. Liu, H. Zhang, W. Tang, H. Xiao, F. Wang, J. Zhu, D. Liu, S. Lin, Y. Zhang, Z. Zhou, C. Chen and H. Liang, *Nanoscale Adv.*, 2022, **4**, 3043–3053.
35 I. Antanaviciute, L. Simatonis, O. Ulcinas, A. Gadeikyte, B. Abakeviciene, S. Tamulevicius, V. Mikalayeva, V. A. Skeberdis, E. Stankevicius and T. Tamulevicius, *J. Tissue Eng. Regener. Med.*, 2018, **12**, e760–e773.
36 C. Akinyi and J. O. Iroh, *Polymers*, 2023, **15**, 299.
37 X. F. Pan, B. Wu, H. L. Gao, S. M. Chen, Y. Zhu, L. Zhou, H. Wu and S. H. Yu, *Adv. Mater.*, 2022, **34**, e2105299.
38 B. Rubehn and T. Stieglitz, *Biomaterials*, 2010, **31**, 3449–3458.
39 S. Ong, A. Kullmann, S. Mertens, D. Rosa and C. A. Diaz-Botia, *Micromachines*, 2022, **13**, 1798.
40 C. Bohler, M. Vomero, M. Soula, M. Voroslakos, M. Porto Cruz, R. Liljemalm, G. Buzsaki, T. Stieglitz and M. Asplund, *Adv. Sci.*, 2023, **10**, e2207576.
41 A. Kilias, Y. T. Lee, U. P. Froriep, C. Sielaff, D. Moser, T. Holzhammer, U. Egert, W. Fang, O. Paul and P. Ruther, *J. Neural. Eng.*, 2021, **18**, 066026.
42 M. Vomero, F. Ciarpella, E. Zucchini, M. Kirsch, L. Fadiga, T. Stieglitz and M. Asplund, *Biomaterials*, 2022, **281**, 121372.
43 T. Boretius, J. Badia, A. Pascual-Font, M. Schuettler, X. Navarro, K. Yoshida and T. Stieglitz, *Biosens. Bioelectron.*, 2010, **26**, 62–69.
44 E. Otte, A. Vlachos and M. Asplund, *Cell Tissue Res.*, 2022, **387**, 461–477.
45 Y. Sun, S. P. Lacour, R. A. Brooks, N. Rushton, J. Fawcett and R. E. Cameron, *J. Biomed. Mater. Res., Part A*, 2009, **90**, 648–655.
46 W. Ma, Y. Ding, M. Zhang, S. Gao, Y. Li, C. Huang and G. Fu, *J. Hazard. Mater.*, 2020, **384**, 121476.

47 Y. Liang, M. Ernst, F. Brings, D. Kireev, V. Maybeck, A. Offenhausser and D. Mayer, *Adv. Healthcare Mater.*, 2018, **7**, e1800304.
48 M. Voisin, M. Ball, C. O'Connell and R. Sherlock, *Nanomedicine*, 2010, **6**, 35–43.
49 G. Abagnale, M. Steger, V. H. Nguyen, N. Hersch, A. Sechi, S. Joussen, B. Denecke, R. Merkel, B. Hoffmann, A. Dreser, U. Schnakenberg, A. Gillner and W. Wagner, *Biomaterials*, 2015, **61**, 316.
50 Q. Fang, J. Wang, S. Gu, R. B. Kaspar, Z. Zhuang, J. Zheng, H. Guo, S. Qiu and Y. Yan, *J. Am. Chem. Soc.*, 2015, **137**, 8352–8355.
51 M. Kowalczuk, Intrinsically Biocompatible Polymer Systems, *Polymers*, 2020, **12**, 272.
52 R. R. Richardson Jr, J. A. Miller and W. M. Reichert, *Biomaterials*, 1993, **14**, 627–635.
53 D. Serbezeanu, T. Vlad-Bubulac, D. Rusu, G. G. Pircalabioru, I. Samoila, S. Dinescu and M. Aflori, *Materials*, 2019, **12**, 3201.
54 S. Nagaoka, K. Ashiba and H. Kawakami, *Artif. Organs*, 2002, **26**, 670–675.
55 P. Starr, C. M. Agrawal and S. Bailey, *J. Biomed. Mater. Res., Part A*, 2016, **104**, 406–412.
56 A. M. Feldweg, D. S. Friend, J. S. Zhou, Y. Kanaoka, M. Daheshia, L. Li, K. F. Austen and H. R. Katz, *Eur. J. Immunol.*, 2003, **33**, 2262–2268.
57 L. I. Buruiana, A. I. Barzic, I. Stoica and C. Hulubei, *J. Polym. Res.*, 2016, **23**, 217.
58 A. Kullmann, D. Kridner, S. Mertens, M. Christianson, D. Rosa and C. A. Diaz-Botia, *Front. Neurosci.*, 2022, **16**, 876877.
59 J. H. Lass, B. A. Benetz, J. He, C. Hamilton, M. Von Tress, J. Dickerson and S. Lane, *Am. J. Ophthalmol.*, 2019, **208**, 211–218.
60 E. Efsa Panel on Food Contact Materials, and Processing, V. Silano, J. M. B. Baviera, C. Bolognesi, A. Chesson, P. S. Cocconcelli, R. Crebelli, D. M. Gott, K. Grob, C. Lambre, E. Lampi, M. Mengelers, A. Mortensen, I. L. Steffensen, C. Tlustos, H. Van Loveren, L. Vernis, H. Zorn, L. Castle, E. Di Consiglio, R. Franz, N. Hellwig, M. R. Milana, K. Pfaff, K. Volk and G. Riviere, *EFSA J.*, 2020, **18**, e06183.
61 C. Y. Lin, W. S. Lou, J. C. Chen, K. Y. Weng, M. C. Shih, Y. W. Hung, Z. Y. Chen and M. C. Wang, *Micromachines*, 2020, **11**, 1064.
62 L. J. Shen, Y. Q. Chen, D. Cheng, C. Zhang, L. Jiang, M. Hong and Q. Y. Kang, *Curr. Eye Res.*, 2016, **41**, 79–87.
63 K. H. Nam, M. Abdulhafez, E. Castagnola, G. N. Tomaraei, X. T. Cui and M. Bedewy, *Carbon*, 2022, **188**, 209–219.
64 M. E. E. Alahi, Y. Liu, S. Khademi, A. Nag, H. Wang, T. Wu and S. C. Mukhopadhyay, *Biosensors*, 2022, **12**, 1044.
65 U. J. Jeong, J. Lee, N. Chou, K. Kim, H. Shin, U. Chae, H. Y. Yu and I. J. Cho, *Lab Chip*, 2021, **21**, 2383–2397.
66 M. Lee, D. Kim, H. S. Shin, H. G. Sung and J. H. Choi, *J. Vis. Exp.*, 2011, e2562.
67 Y. Tchoe, T. Wu, U. Hoi Sang, D. M. Roth, D. Kim, J. Lee, D. R. Cleary, P. Pizarro, K. J. Tonsfeldt, K. Lee, P. C. Chen, A. M. Bourhis, I. Galton, B. Coughlin, J. C. Yang, A. C. Paulk, E. Halgren, S. S. Cash and S. A. Dayeh, *bioRxiv*, 2023, preprint, DOI: **10.1101/2023.07.19.549735**.
68 M. Komatsu, E. Sugano, H. Tomita and N. Fujii, *Front. Neurosci.*, 2017, **11**, 514.
69 M. McAvoy, J. K. Tsosie, K. N. Vyas, O. F. Khan, K. Sadtler, R. Langer and D. G. Anderson, *Theranostics*, 2019, **9**, 7099–7107.
70 P. M. Rossini, S. Micera, A. Benvenuto, J. Carpaneto, G. Cavallo, L. Citi, C. Cipriani, L. Denaro, V. Denaro, G. Di Pino, F. Ferreri, E. Guglielmelli, K. P. Hoffmann, S. Raspopovic, J. Rigosa, L. Rossini, M. Tombini and P. Dario, *Clin. Neurophysiol.*, 2010, **121**, 777–783.
71 R. Herbert, S. Mishra, H. R. Lim, H. Yoo and W. H. Yeo, *Adv. Sci.*, 2019, **6**, 1901034.
72 B. Panda, S. Mandal and S. J. A. Majerus, *IEEE Trans. Biomed. Circuits Syst.*, 2019, **13**, 1494–1505.
73 R. Lin, Y. Jin, R. R. Li, C. Jiang, J. Ping, C. J. Charles, Y. L. Kong and J. S. Ho, *Biosens. Bioelectron.*, 2022, **216**, 114651.
74 J. Guo, A. E. N. Asli, K. R. Williams, P. L. Lai, X. Wang, R. Montazami and N. N. Hashemi, *Biosensors*, 2019, **9**, 112.
75 P. S. Tan, E. Vaughan, J. Islam, N. Burke, D. Iacopino and J. B. Tierney, *Nanomaterials*, 2021, **11**(8), 2110.
76 S. Nesson, M. Yu, X. Zhang and A. H. Hsieh, *J. Biomed. Opt.*, 2008, **13**, 044040.
77 J. J. Kim, G. R. Stafford, C. Beauchamp and S. A. Kim, *Sensors*, 2020, **20**, 3953.
78 Z. J. Wu, Z. Luo, A. Rastogi, S. Stavchansky, P. D. Bowman and P. S. Ho, *Biomed. Microdevices*, 2011, **13**, 485–491.
79 D. A. Borkholder, X. Zhu and R. D. Frisina, *J. Controlled Release*, 2014, **174**, 171–176.
80 A. Santillan, D. G. Rubin, C. P. Foley, D. Sondhi, R. G. Crystal, Y. P. Gobin and D. J. Ballon, *J. Neurosci. Methods*, 2014, **222**, 106–110.
81 N. Unver, S. Odabas, G. B. Demirel and O. T. Gul, *J. Mater. Chem. B*, 2022, **10**, 8419–8431.
82 B. J. Lyon, A. I. Aria and M. Gharib, *Biomed. Microdevices*, 2014, **16**, 879–886.
83 F. Teodorescu, G. Queniat, C. Foulon, M. Lecoeur, A. Barras, S. Boulahneche, M. S. Medjram, T. Hubert, A. Abderrahmani, R. Boukherroub and S. Szunerits, *J. Controlled Release*, 2017, **245**, 137–146.
84 Q. Pagneux, R. Ye, L. Chengnan, A. Barras, N. Hennuyer, B. Staels, D. Caina, J. I. A. Osses, A. Abderrahmani, V. Plaisance, V. Pawlowski, R. Boukherroub, S. Melinte and S. Szunerits, *Nanoscale Horiz.*, 2020, **5**, 663–670.
85 R. Kaewmanee, F. Wang, Y. Pan, S. Mei, J. Meesane, F. Li, Z. Wu and J. Wei, *Biomater. Sci.*, 2022, **10**, 4243–4256.
86 Y. Zhang, W. Jiang, S. Yuan, Q. Zhao, Z. Liu and W. Yu, *Int. J. Nanomed.*, 2020, **15**, 9389–9405.
87 R. Kaewmanee, F. Wang, S. Mei, Y. Pan, B. Yu, Z. Wu, J. Meesane and J. Wei, *J. Mater. Chem. B*, 2022, **10**, 5058–5070.
88 Y. Ling, W. Pang, J. Liu, M. Page, Y. Xu, G. Zhao, D. Stalla, J. Xie, Y. Zhang and Z. Yan, *Nat. Commun.*, 2022, **13**, 524.
89 M. Mariello, A. Qualtieri, G. Mele and M. De Vittorio, *ACS Appl. Mater. Interfaces*, 2021, **13**, 20606–20621.

90 H. Zhong, Z. Zhu, P. You, J. Lin, C. F. Cheung, V. L. Lu, F. Yan, C. Y. Chan and G. Li, *ACS Nano*, 2020, **14**, 8846–8854.
91 D. U. Lee, D. W. Kim, S. Y. Lee, D. Y. Choi, S. Y. Choi, K. S. Moon, M. Y. Shon and M. J. Moon, *Colloids Surf., B*, 2022, **211**, 112314.
92 Q. Li, J. Li, G. Liao and Z. Xu, *J. Mater. Sci.: Mater. Med.*, 2018, **29**, 126.
93 X. Strakosas, H. Biesmans, T. Abrahamsson, K. Hellman, M. S. Ejneby, M. J. Donahue, P. Ekstrom, F. Ek, M. Savvakis, M. Hjort, D. Bliman, M. Linares, C. Lindholm, E. Stavrinidou, J. Y. Gerasimov, D. T. Simon, R. Olsson and M. Berggren, *Science*, 2023, **379**, 795–802.
94 Z. Zhao, H. Zhu, X. Li, L. Sun, F. He, J. E. Chung, D. F. Liu, L. Frank, L. Luan and C. Xie, *Nat. Biomed. Eng.*, 2023, **7**, 520–532.
95 T. K. Nguyen, M. Barton, A. Ashok, T. A. Truong, S. Yadav, M. Leitch, T. V. Nguyen, N. Kashaninejad, T. Dinh, L. Hold, Y. Yamauchi, N. T. Nguyen and H. P. Phan, *Proc. Natl. Acad. Sci. U. S. A.*, 2022, **119**, e2203287119.
96 C. E. Cruttenden, J. M. Taylor, S. Hu, Y. Zhang, X. H. Zhu, W. Chen and R. Rajamani, *Biomed. Phys. Eng. Express*, 2017, **4**, 015001.
97 S. H. Bae, J. H. Che, J. M. Seo, J. Jeong, E. T. Kim, S. W. Lee, K. I. Koo, G. J. Suaning, N. H. Lovell, D. I. Cho, S. J. Kim and H. Chung, *Invest. Ophthalmol. Vis. Sci.*, 2012, **53**, 2653–2657.
98 S. Srinivasan, K. Vyas, M. McAvoy, P. Calvaresi, O. F. Khan, R. Langer, D. G. Anderson and H. Herr, *Front. Neurol.*, 2019, **10**, 252.
99 X. Xuan, H. S. Yoon and J. Y. Park, *Biosens. Bioelectron.*, 2018, **109**, 75–82.
100 Y. Zhu, P. Xia, J. Liu, Z. Fang, L. Du and Z. Zhao, *Micromachines*, 2022, **13**, 75–82.
101 H. U. Kim, H. Y. Kim, H. Seok, V. Kanade, H. Yoo, K. Y. Park, J. H. Lee, M. H. Lee and T. Kim, *Anal. Chem.*, 2020, **92**, 6327–6333.
102 N. R. Shanmugam, S. Muthukumar, S. Chaudhry, J. Anguiano and S. Prasad, *Biosens. Bioelectron.*, 2017, **89**, 764–772.
103 I. Shitanda, T. Oshimoto, N. Loew, M. Motosuke, H. Watanabe, T. Mikawa and M. Itagaki, *Biosens. Bioelectron.*, 2023, **238**, 115555.
104 Y. Tian, Y. Liu, Y. Wang, J. Xu and X. Yu, *Sensors*, 2021, **21**, 118.
105 A. Rastogi, P. D. Bowman and S. Stavchansky, *Drug Delivery Transl. Res.*, 2012, **2**, 106–111.
106 S. Metz, A. Bertsch, D. Bertrand and P. Renaud, *Biosens. Bioelectron.*, 2004, **19**, 1309–1318.
107 Y. Hu, Y. Wang, Q. Feng, T. Chen, Z. Hao, S. Zhang, L. Cai, X. Guo and J. Li, *Biomater. Sci.*, 2023, **11**, 3486–3501.
108 F. S. L. Bobbert, K. Lietaert, A. A. Eftekhari, B. Pouran, S. M. Ahmadi, H. Weinans and A. A. Zadpoor, *Acta Biomater.*, 2017, **53**, 572–584.
109 A. J. T. Teo, A. Mishra, I. Park, Y. J. Kim, W. T. Park and Y. J. Yoon, *ACS Biomater. Sci. Eng.*, 2016, **2**, 454–472.
110 S. Asadullah, S. Mei, K. Yang, X. Hu, F. Wang, B. Yu, Z. Wu and J. Wei, *J. Mech. Behav. Biomed. Mater.*, 2021, **124**, 104800.
111 N. El-Atab, N. Qaiser, H. Badghaish, S. F. Shaikh and M. M. Hussain, *ACS Nano*, 2020, **14**, 7659–7665.
112 M. Loeb, A. Bartholomew, M. Hashmi, W. Tarhuni, M. Hassany, I. Youngster, R. Somayaji, O. Larios, J. Kim, B. Missaghi, J. V. Vayalumkal, D. Mertz, Z. Chagla, M. Cividino, K. Ali, S. Mansour, L. A. Castellucci, C. Frenette, L. Parkes, M. Downing, M. Muller, V. Glavin, J. Newton, R. Hookoom, J. A. Leis, J. Kinross, S. Smith, S. Borhan, P. Singh, E. Pullenayegum and J. Conly, *Ann. Intern. Med.*, 2022, **175**, 1629–1638.
113 F. Topuz, M. A. Abdulhamid, R. Hardian, T. Holtzl and G. Szekely, *J. Hazard. Mater.*, 2022, **424**, 127347.
114 H. W. Chen, Y. L. Kuo, C. H. Chen, C. S. Chiou, W. T. Chen and Y. H. Lai, *Process Saf. Environ. Prot.*, 2022, **167**, 695–707.
115 B. Ghatak, S. Banerjee, S. B. Ali, R. Bandyopadhyay, N. Das, D. Mandal and B. Tudu, *Nano Energy*, 2021, **79**, 105387.
116 W. Ma, Y. Li, M. Zhang, S. Gao, J. Cui, C. Huang and G. Fu, *ACS Appl. Mater. Interfaces*, 2020, **12**, 34999–35010.
117 E. A. Cuello, L. E. Mulko, C. A. Barbero, D. F. Acevedo and E. I. Yslas, *Colloids Surf., B*, 2020, **188**, 110801.
118 R. Eivazzadeh-Keihan, Z. Sadat, A. Mohammadi, H. A. M. Aliabadi, A. Kashtiaray, A. Maleki and M. Mahdavi, *Sci. Rep.*, 2023, **13**, 9598.